

Demand Response Under the Smart Grid Paradigm

M. Negnevitsky

School of Engineering and ICT, University of Tasmania, Australia
E-mail: Michael.Negnevitsky@utas.edu.au

Abstract -

Electric power industry is undergoing a profound change. The change is driven by technical, economic and environmental factors. The emerging challenges are particularly significant for distribution grids, where the level of automation or “smartness” is relatively low. With the push for energy conservation, demand-side management (DSM) and demand response (DR) are becoming vital tools under the smart grid paradigm. This paper outlines some experience obtained at the University of Tasmania, Australia in developing DSM and DR systems.

Keywords -

Smart Grid; Distribution System; Demand-side Management; Demand Response.

1 Introduction

Electric power systems are undergoing a profound change. This change is driven by several factors that include technical, economic and environmental factors. We need to deal with an aging infrastructure of power systems and maintain the required level of grid reliability. We need to integrate renewable energy sources, particularly wind and solar, and provide secure power supply to our customers, and at the same time improve operational efficiency. The emerging changes and challenges are particularly significant for distribution grids, where the level of automation or “smartness” is relatively low. Manual and “blind” operations along with old electromechanical relays are to be transformed into a “smart grid”. This transformation is necessary to meet environmental targets, accommodate distributed generation, and support plug-in electric vehicles. In fact, these needs present the power industry with the biggest challenge it has ever faced. On one hand, the transition to the “grid of the future” has to be evolutionary – we still need to supply electricity to our customers to keep the lights on. On the other hand, the challenges associated with the smart grid are significant enough to expect revolutionary changes in power system design and operation.

With the push for energy conservation, demand-side

management and demand response are becoming vital tools under the broad smart grid paradigm.

The term “demand-side management” (DSM) was first introduced by Electric Power Research Institute (EPRI) in the 1980s, and since then has been widely used around the world. In fact, DSM is a term that implies many activities such as direct load control, peak shaving, peak shifting, and various load management strategies. Effective load management programs are often referred to as demand response (DR). According to the US Federal Energy Regulatory Commission, DR is defined as:

“Changes in electric usage by end-use customers from their normal consumption patterns in response to changes in the price of electricity over time, or to incentive payments designed to induce lower electricity use at times of high wholesale market prices or when system reliability is jeopardized.”

This paper outlines some experience obtained at the University of Tasmania, Australia in developing DSM and DR systems. Section 2 presents an evaluation tool for DSM of domestic hot water systems in distribution grid, and Section 3 discusses the development and implementation of fast DR in isolated power systems.

2 Demand-side Management Evaluation Tool

Effective implementation of DSM programs delivers operational benefits such as reduced peak demands and relieved overloads, which are essential in a power system with growing penetration of fundamentally intermittent renewable energy sources [1]. Successful DSM programs also provide economic gains such as deferrals of costly network upgrades as well as network security enhancements [1]. Moreover, in a deregulated electricity market, DSM programs offer opportunities for aggregation of demand reduction to support market and network operations of a power system [2]. In addition, consumers receive financial incentives through participation in DSM programs.

There are three different methods to implement DSM in a power distribution network. In indirect load control, consumers manually adjust their consumption in response to incentive programs such as time-of-use

(TOU) tariffs [3]. In autonomous load control, devices autonomously adjust their consumption in response to detected changes in the power system or to commands sent from the control centre. In direct load control (DLC), devices are centrally controlled by the utility operator [4].

Hot water load forms a significant share of the total domestic demand. For example, it accounts for up to 40% of domestic energy consumption in Australia, and around one third in Tasmania [5], [6]. Moreover, domestic hot water systems represent insulated thermal energy storages that continually supply hot water even during periods of power interruption. Hence, they are commonly targeted for DSM programs to reduce peak loads and improve the load factor. Well-designed DSM programs minimize customer discomfort due to cold showers.

This section presents the development of an evaluation tool that assists in designing a DSM program to deliver desired peak load reductions while maintaining satisfactory level of comfort for all customers. The tool estimates the available domestic hot water loads in a controlled area, and determines optimal switching programs. A switching program refers to a direct load control schedule applied to domestic hot water systems (to strategically switch them on and off) in order to achieve a desired load reduction during peak periods.

2.1 Structure of the Tool

Main modules of the tool are shown in Figure 1. The modules are grouped in three main functional blocks. The numbered grey circles represent inputs and outputs (I/O).

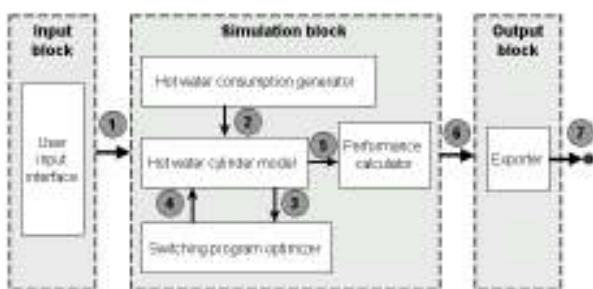


Figure 1. The structure of the DSM evaluation tool.

The Input block represents the user interface, which allows the tool user to enter parameters required for simulation (the number of households in the controlled area, the number of Monte Carlo simulations, the desired peak reduction, etc.) as well as to view default parameters and change them if necessary. The

Simulation block is the main block of the tool; it contains four modules: the hot water consumption generator, hot water cylinder model, switching program optimizer, and performance calculator. The Output block contains the exporter, which exports the data to an external (Excel) file.

Default parameters and parameters entered by the user via the user input interface are represented by I/O 1. The hot water consumption generator receives I/O 1 and determines hot water consumption profiles for individual households; these profiles are represented by I/O 2. The hot water cylinder model receives I/O 2 and calculates uncontrolled hot water loads and shower temperatures for the households; the results are represented by I/O 3. The user can observe the aggregate uncontrolled load curve of the households in the controlled area, and proceed with the optimization of switching programs. The switching program optimizer receives I/O 3 and produces switching programs based on the user-defined parameters (the desired peak reduction target, control periods etc.). The best switching programs are presented to the user, so that he/she can select the most suitable switching program. The hot water cylinder model then calculates controlled hot water loads (I/O 5) by applying the user-selected switching program (I/O 4) to the hot water consumption profiles (I/O 2). The performance calculator receives I/O 5 and determines key performance indicators such as peak reductions and customer's comfort. Results in the form of 24-hour load curves are presented to the user (I/O 6), and exported to an external file (I/O 7) via the exporter.

2.2 Hot Water Consumption Generator

The first step in the development of the hot water consumption generator was to acquire knowledge of hot water consumption patterns of households in the controlled area. To achieve this objective, a telephone survey was conducted on 1000 randomly selected households across Tasmania. It recorded demographic data (e.g. number of usual residents, combined income etc.) and details of hot water usages (e.g. average number of showers per day, average shower length etc.) of the surveyed households. This survey focused on two peak periods in the Tasmanian power distribution network, i.e. morning and evening peaks from 6am to 10am and from 5pm to 8pm, respectively. Figure 2 and Figure 3 show major results of the survey. Figure 2 suggests a positive correlation between the average number of showers and the family size, in the morning and evening peaks. An unexpected drop in the average number of morning showers in households with six or more residents can be explained by a relatively small

sample size of this household type (just 2.3% of the total surveyed households).

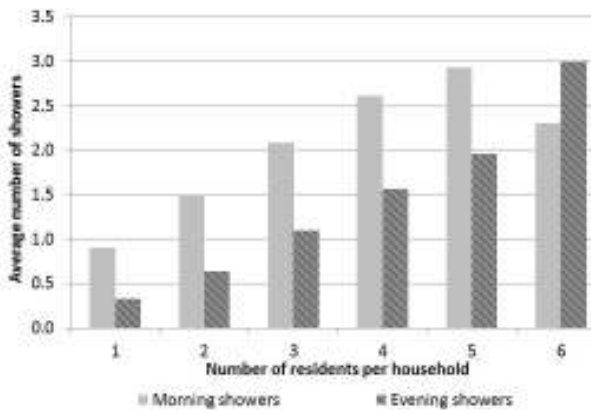


Figure 2. The average number of showers versus family size.

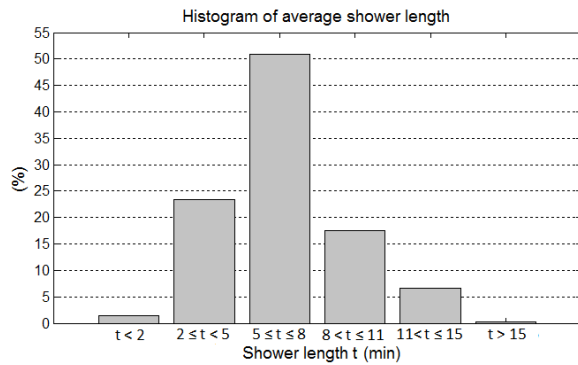


Figure 3. The histogram of average lengths of showers.

As can be seen in Figure 3, the length of a shower can vary from 2 min to 15 min, however, a great majority of showers (about 51%) last from 5 min to 8 min.

To estimate domestic hot water consumption profiles, we also acquired energy metering data of 279 households across Tasmania. These data were obtained from meters dedicated for metering electric water heating alone, and represented water heating energy consumption of individual households recorded in 5-minute intervals. We considered two types of hot water usages: high volume usage that lasts for more than 5 min and low volume usage that lasts for 5 min or less. Based on the modelling, 1 min of hot water usage requires approximately 10 min of heating to restore the temperature set by the thermostat. Thus, a continuous energy consumption (a switched-on condition of the electric water heater) for a period of more than 50 min is regarded as a high volume usage (represented by showers), and a consumption of less than or equal to 50

min is regarded as a low volume usage. Using weekday data only, we derived probability distributions of the starting time for showers (Figure 4) and low volume usages (Figure 5).

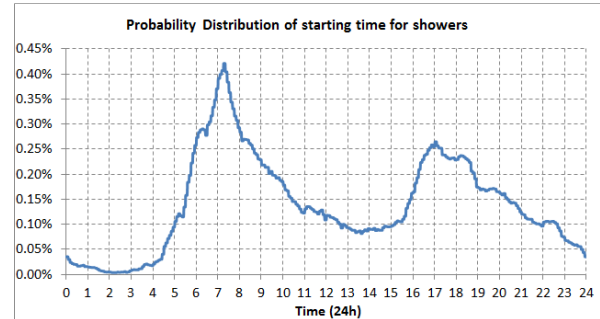


Figure 4. The probability distribution of the shower starting time.

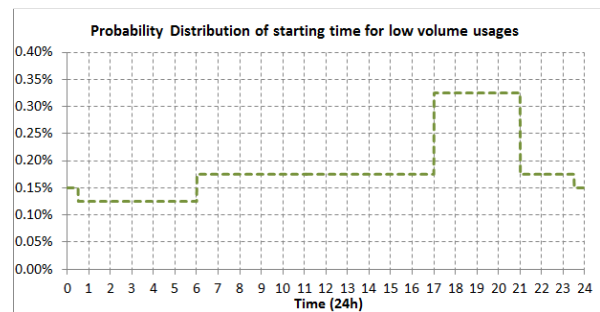


Figure 5. Probability distribution of the starting time for low volume usages.

Both survey results and energy metering data revealed that domestic hot water consumption depends mostly on the family size. Therefore, all households in a controlled area are divided into four groups according to the family type based on the number of residents in a household. Table 1 shows a typical distribution of families in a controlled area.

We need also specify probabilities of household occupants taking morning showers only, evening showers only, or both. Demographic data [7] and household energy consumption records are used to estimate probabilities in Table 2, which determine the number of showers each family type take in the morning, evening, or morning and evening. Similar to showers, the probability of a low volume usage depends on the family size of a household. The tool uses multipliers to scale this probability up based on the family type. Default values of the multipliers are 1.0, 1.2, 1.6 and 2.0, respectively. The tool user can redefine these values, if required. Figure 5 gives the probability of a low volume usage occurring in a household at a given time.

Shower lengths and gaps between consecutive showers are specified by their mean, maximum and minimum values. We define minimum and maximum to discard unrealistic values (e.g., a one-minute shower) in probabilistic simulations. Normal distributions are assumed. Default values used by the tool are shown in Table 3. A low volume usage is denoted as a single 5-min draw. If required, the user can redefine these values.

Table 1: Family types and their distributions

Family Type	1	2	3	4
Family size	Very small	Small	Average	Large
Number of residents	1	2 to 3	4 to 5	6 and above
Distribution in a population	25%	50%	22.5%	2.5%

Table 2: Shower probabilities for different families

Family type	Number of shower					
	0	1	2	3	4	5
Type 1	5%	95%	0%	0%	0%	0%
Type 2	0%	41%	53%	6%	0%	0%
Type 3	0%	20%	60%	19%	1%	0%
Type 4	0%	7%	40%	47%	5%	1%

Table 3: Shower lengths and gaps between showers

Parameter	Min (min)	Max (min)	Mean (min)	Standard deviation (min)
Shower length	5	15	8	4
Shower gap	5	7	6	1

The starting time of each hot water usage is specified based on probability distributions derived from actual energy metering data.

The tool employs a Monte Carlo approach to generate hot water consumption profiles for each household. First, the tool generates random values to determine specific parameters for a single household: family type, when showers are taken (morning, or evening, or morning and evening), number of showers, number of low volume usages, length of each shower and each gap between consecutive showers, starting time for each shower and each low volume usage. Next, using these parameters, the tool generates a 24-hour hot water consumption profile for a single household. The tool then repeats the profile generation process for a specified number of households using a new set of random values each time. Finally, the whole process is repeated for the required number of Monte Carlo iterations. Based on the generated hot water profiles, we can now proceed with calculating loads associated with household hot water usages. However, we need to develop a hot water cylinder model first.

2.3 Hot Water Cylinder Model

The block diagram of a DEHW system with a single

heating element is shown in Figure 6.

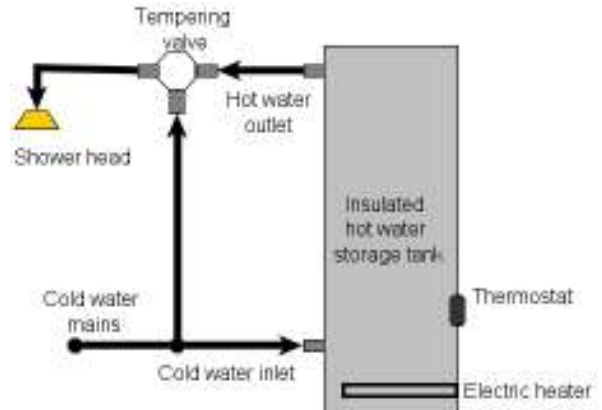


Figure 6. Block diagram of a domestic electric hot water system.

For predicting the shower temperature and power consumption for domestic hot water systems accurately, we develop a hot water cylinder model based on the most common domestic hot water system in Tasmania, which has a 165 L cylindrical storage tank and a single 2.4 kW heating element. We validated the model with experimental data and found that predicted and measured values were closely matched. The measured and predicted values of normalized power consumption and top layer temperature over 48 hours are shown in Figure 7 and Figure 8. Figure 9 shows the measured and predicted shower temperatures during four successive showers.

We found that the mean prediction error in the total energy consumption was less than 6%, while the mean absolute error in predicted shower temperature was less than 3°C. It was considered acceptable for the model to be used in the tool.

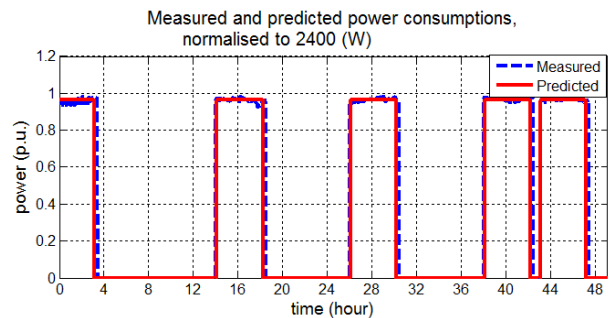


Figure 7. Measured and predicted power consumptions, normalised to 2400 (W).

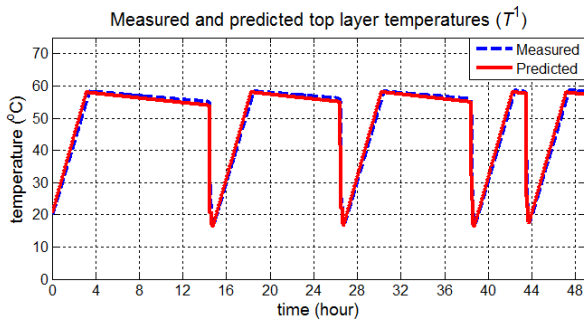


Figure 8. Measured and predicted top layer temperatures of the storage tank.

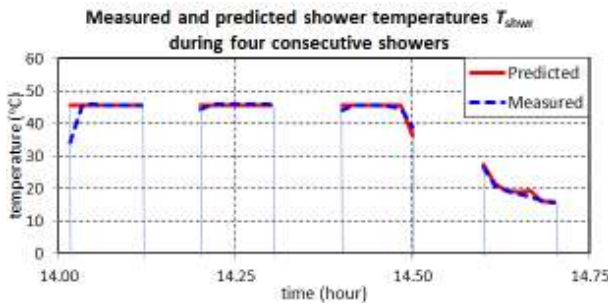


Figure 9. Measured and predicted shower temperatures in a shower schedule.

2.4 Performance calculator

The performance calculator has two main functions: calculating peak reductions in the hot water load and estimating the customers comfort level.

First, it determines an average uncontrolled load profile for each household. The average uncontrolled load profile for a household represents an average profile of the household obtained over a specified number of Monte Carlo iterations.

Then, it determines an aggregate uncontrolled load curve L_U by aggregating uncontrolled load profiles for all households. An aggregate controlled load curve L_C is obtained in a similar manner after a switching program is applied to the uncontrolled loads produced by the hot water cylinder model for individual households. The peak load reduction R_τ of the control period τ is defined as

$$R_\tau = 1 - \frac{\max[L_C(\tau)]}{\max[L_U(\tau)]} \quad (1)$$

where $\max[L_C(\tau)]$ and $\max[L_U(\tau)]$ are the peaks of L_C and L_U the control period τ , respectively.

The customer's comfort level depends on the frequency (or probability) of getting a "cold shower"—the event when the shower temperature drops below the comfort temperature (e.g. 43°C) specified by the tool user. Preferred shower temperatures range from 40°C to 44°C [8]. Because of a large number of households in the controlled area, we can assume the same comfort

temperature for all customers. The tool allows the user to change the comfort temperature if required.

2.5 Switching Program Optimization

Figure 10 shows a block diagram of the switching program optimizer. Here I/Os are depicted as numbered blocks. I/O 1 represents parameters of the control management system, I/O 2 optimization parameters, I/O 3 uncontrolled loads generated by the hot water cylinder model, and I/O 4 represents optimized switching programs.

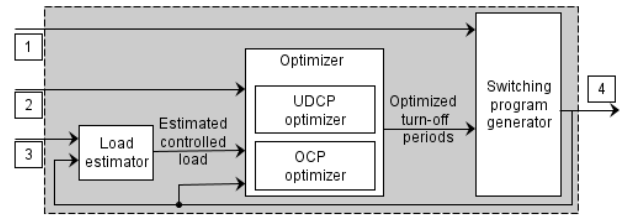


Figure 10. The block diagram of the switching program optimizer.

The switching program generator uses user-specified control management system parameters and optimized turn-off periods from the optimizer to create switching programs, as shown in Figure 11. Here a control step is the smallest switching time interval, and a turn-off period is the time interval where the hot water system is turned off for a number of consecutive control steps. A switching cycle consists of the turn-off period followed by the turn-on period. A control period consists of multiple switching cycles (there are two control periods – for the morning peak and for the evening peak). Control groups are formed by shifting the switching cycles by one or more control steps. To ensure the time-shifted switching cycles are contained within a control period, each control group has one switching cycle less than the control period. In [9], it was demonstrated that division of households based on the family type does not significantly affect the comfort level of household residents. Therefore, the entire set of households can be divided into control groups of approximately the same size regardless of the family type of a household.

The load estimator determines the total controlled hot water load by applying a switching program to uncontrolled loads of individual households. The load estimator sets the load to zero during the turn-off periods of the applied switching program and restores the load during the turn-on periods. Water temperature is not considered in the load estimation.

The main function of the optimizer is to optimize turn-off periods of a switching program. It consists of the user-defined control period (UDCP) optimizer and the optimized control period (OCP) optimizer.

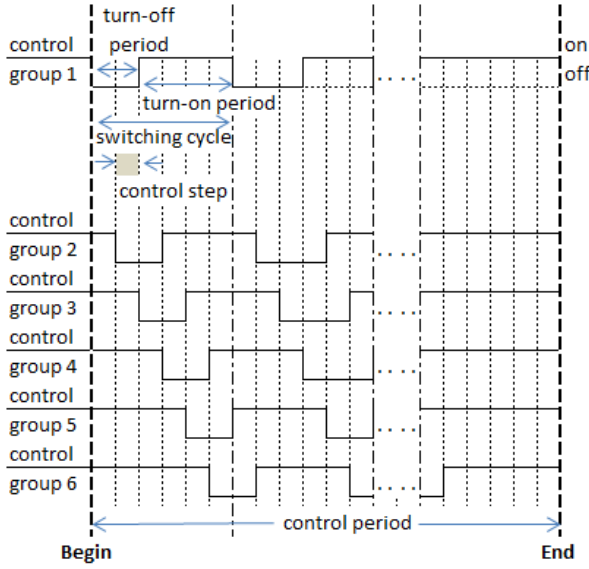


Figure 11. A switching program and its control management system parameters.

The UDCP optimizer determines turn-off periods based on the user-defined control periods and the peak load reduction targets. The control periods remain unchanged throughout the optimization process. The UDCP optimizer implements an iterative process to minimize the mean error between the user-defined target L_T and the estimated aggregate controlled load L_C in each switching cycle of a switching program. To calculate required changes in the turn-off period for each switching cycle, it applies proportional and integral (PI) functions to the errors. In Figure 12, $e(j,k)$ and $\tau_{\text{off}}(j,k)$ are the mean error and the turn-off period of switching cycle j in iteration k , respectively; K_p is the proportional gain and T_i the integral time of the PI functions.

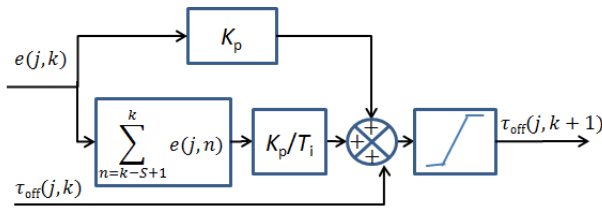


Figure 12. Block diagram of the UDCP optimizer.

The proportional function multiplies the error by K_p . The integral function sums the errors of switching cycle j from the previous $(S-1)$ iterations to the current one, and multiplies the result by K_p/T_i . The sum of the current turn-off period and outputs from PI functions is converted by the limiter function into an integer

between the minimum and maximum values. The final result is the turn-off period for the next iteration.

The OCP optimizer determines turn-off periods and control periods of a switching program based on the user-defined peak load reduction target L_T . First, it finds the starting time t_s and finishing time t_f of the initial control period. The time t_s is found as the first intersection of the aggregate uncontrolled load L_U and the target L_T , as shown in Figure 13. To avoid a high payback peak after the control period, the finishing time t_f is found by solving the following equation:

$$\int_{t_s}^{t_f} L_U(t) \cdot dt = L_T \cdot (t_s - t_f) \quad (2)$$

where the left hand term represents the total uncontrolled energy consumption between t_s and t_f .

To further minimize the error between L_C and L_T , the OCP optimizer iteratively tunes the switching program optimized by the UDCP optimizer. The OCP optimizer increases or decreases the turn-off period τ_{off} of each switching cycle to minimize the error between L_T and L_C . We define three tolerance levels: L_1 and L_2 are, respectively, 1% and 2% above L_T , and $L_3(j)$ is the difference between L_T and the estimated maximum restored load in switching cycle j , if $\tau_{\text{off}}(j)$ is decreased by one control step:

$$L_3(j) = L_T - \max[L_U(j-2), L_U(j-1), L_U(j)] \cdot \frac{\tau_{\text{step}}}{\tau_{\text{sc}}} \quad (3)$$

where τ_{step} is the control step; τ_{sc} is the switching cycle; $\max[L_U(j-2), L_U(j-1), L_U(j)]$ is the maximum value of the aggregate uncontrolled load L_U over three switching cycles $(j-2)$, $(j-1)$ and j .



Figure 13. Initial control period in relation to L_T and L_U .

The OCP optimizer tunes the τ_{off} of all but the last switching cycle within a control period based on the three scenarios shown below, where $L_C(j)$ denotes values of L_C within switching cycle j .

- Scenario 1. The peak of $L_C(j)$ is above L_2 .
- Scenario 2. $L_C(j)$ stays between L_1 and L_2 for more than 15 min.
- Scenario 3. The peak of $L_C(j)$ is below $L_3(j)$.

Scenarios 1 and 2 represent overshooting, whereas Scenario 3 indicates over-control that can potentially create higher payback peaks. The OCP optimizer reduces $L_C(j)$ by increasing $\tau_{\text{off}}(j)$ by one τ_{step} , if either Scenario 1 or Scenario 2 is met. If Scenario 3 is met, $\tau_{\text{off}}(j)$ is decreased by one τ_{step} . No change is made on $\tau_{\text{off}}(j)$ if none of the above conditions are met.

Before changing $\tau_{\text{off}}(j)$, the OCP optimizer considers the current value of τ_{off} (expressed as the number of control steps) and the location of the peak of $L_C(j)$ within switching cycle j . For a peak located within control step n of the switching cycle, increasing τ_{off} of this switching cycle will reduce the peak only if the current value of τ_{off} is below or equal to $(n-1)$; decreasing τ_{off} of this switching cycle will increase the peak only if the current value of τ_{off} is below or equal to n .

If j is the last switching cycle of a control period, and either Scenario 1 or Scenario 2 is met, the control period is extended by one switching cycle; $\tau_{\text{off}}(j)$ is then set to a value equal to a multiple of τ_{step} and proportional to the error between the peak of $L_C(j)$ and L_T . Through iterations, the OCP optimizer tunes the switching program so that the aggregate controlled load stays below or as close as possible to the user-defined target.

2.6 Case Studies

We conducted several case studies to evaluate the performance of the DSM evaluation tool under various scenarios for 279 households. This set of households provided us the opportunity to use actual energy metering data in the developed tool. We used the tool to randomly generate hot water consumption profiles for 279 households and obtained an aggregate uncontrolled hot water load curve, which matched the actual data. In case studies 1 and 2, we investigated potential impacts of using constant values of ambient temperature, cold water temperature and thermostat settings on the simulation results. In subsequent studies, we evaluated the performance of switching programs produced by the optimizer in terms of the peak load reduction and customer comfort level. We used 43°C as the preferred shower temperature for all households. The default switching program configuration had 30 min switching cycles and 5 min control steps. The turn-off period in a switching cycle varied from 5 min to 25 min in the 5-minute step. The households were divided into six control groups of almost equal size.

2.6.1 Case Study 1

This case study compares results of two simulations. In the first simulation, we use actual values of ambient temperature T_a and cold water temperatures T_c , shown in Figure 14. Shaded areas indicate peak periods of hot water usage (06:00 – 09:00 and 16:30 – 18:30). The

profile of T_a is obtained from historical climate data for Tasmania [10]; T_c usually has a positive correlation with T_a [11], but has a smaller range of variation. As can be seen in Figure 14, values of T_a and T_c vary considerably over the 24-hour period (particularly, values of T_a), but their variations during peak periods are rather small. Therefore, in the second simulation, T_a and T_c are set to constant value of 8°C.

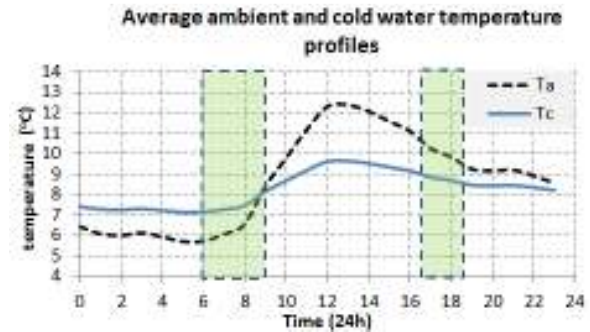


Figure 14. Average ambient and cold water temperatures in winter time.

Figure 15 shows two aggregate uncontrolled hot water load curves obtained using variable and constant values for ambient and cold water temperatures. We find insignificant difference between the two curves. The difference in the total energy consumption is about 1%, and the mean absolute error (MAE) is about 1.3p.u. The results can be explained by the fact that a great majority of hot water usages occur during peak periods when variations of actual cold water temperature are rather small (within $\pm 1^\circ\text{C}$, in shaded areas of Fig. 14). On the other hand, although T_a varies significantly during the day, its variation has negligible overall effect on the rate of hot water tank heat losses. An insulated hot water tank idles for a long period (usually from 13 to 15 hours) between two consecutive recharges due to heat loss. During this period, the effect of T_a variation is smoothed, and the average value of T_a produces similar results as its variable values. Thus, variations of T_a and T_c can be represented with their respective average values in further studies.

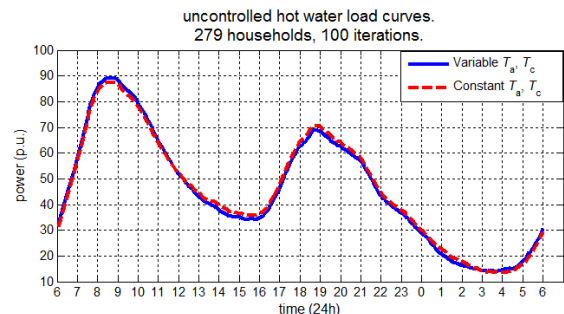


Figure 15. Uncontrolled load curves for constant and variable values of ambient and cold water temperatures.

2.6.2 Case Study 2

This case study compares the performance of the UDCP optimizer and the OCP optimizer. Both use the default switching program configuration to produce optimized switching programs that are applied to the same set of hot water loads. The peak reduction target is 15% in both cases. Figure 16 and Figure 17 show the aggregate controlled load curves produced by the UDCP and OCP optimizers, respectively. Table 4 shows the control periods and peak reductions achieved. The UDCP optimizer keeps user-specified control periods constant in its optimization process. Probabilities of cold showers for each family type are shown in Table 5 – for the uncontrolled scenario, and scenarios controlled by the UDCP-optimized and OCP-optimized switching programs.

Comparing the aggregate controlled load curves produced by both optimizers, we find that the OCP optimizer performs much better in terms of peak load reduction.

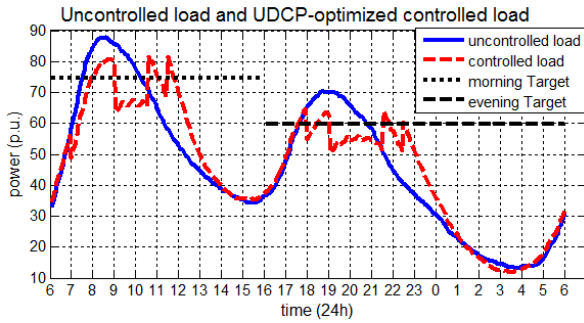


Figure 16. Result of the UDCP optimization.

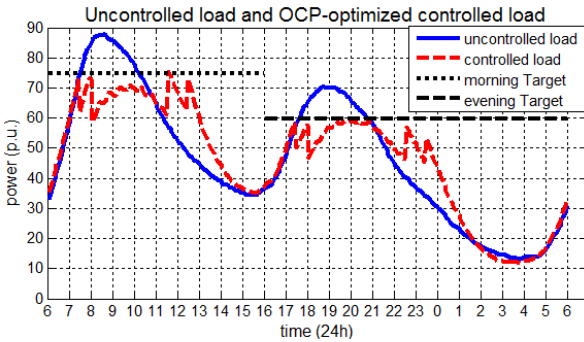


Figure 17. Result of the OCP optimization.

Table 4: Control periods and achieved peak reductions in case study 2

	Morning		Evening	
	Control period	Peak reduction	Control period	Peak reduction
UDCP optimizer	07:00-12:00	7.1%	18:00-23:00	9.3%
OCP optimizer	07:30-13:00	14.3%	17:30-00:00	15.0%

Table 5: Probabilities of cold showers in case study 2

	Uncontrolled	UDCP optimizer	OCP optimizer
Family type 1	0.02%	0.02%	0.03%
Family type 2	4.37%	4.52%	4.63%
Family type 3	7.96%	8.27%	8.44%
Family type 4	13.85%	14.07%	14.36%
Overall	5.06%	5.23%	5.34%

The starting and finishing times of control periods in a switching program are vital for peak load reduction. A delayed control period produces an initial peak above the target line, as in the evening period of Figure 16. Starting a control period too early defers loads needlessly and creates slightly higher peaks in subsequent switching cycles of the same control period, as in the morning control period of Figure 16. Control periods with sufficient length allow a gradual restoration of loads below the target line. Ending a control period prematurely creates an unwanted high payback peak at the end of the control period, as seen at around 11:30 of Figure 16. Similar results were reported in [12] and [13]. Due to shorter than required control periods used for the UDCP optimization, reducing the peaks at 10:30 and 21:30 will produce higher payback peaks at the end of the respective control periods.

While both controlled scenarios produce higher probabilities of cold shower than in the uncontrolled scenario, the OCP optimizer degrades the comfort level more than the UDCP optimizer due to its longer control periods (Table 5).

2.6.3 Case Study 3

In this case study, we evaluate the tool’s ability to optimize switching programs for two different hot water load profiles. The first one has a dominant morning peak (this load profile was used in the case study 3) and the second – a dominant evening peak. The default switching program configuration (30 min switching cycle with 5-minute control steps and six control groups) is used. The peak reduction target is 15%. Figure 18 shows the aggregate uncontrolled load curve of the second hot water load profile, and the aggregate controlled load curve after the OCP-optimized switching program is applied.

Optimized morning and evening control periods are from 07:30 to 15:00 and from 17:30 to 23:30, respectively. A 9.1% peak reduction is achieved for the morning control period, and 13.4% for the evening. Table 6 shows probabilities of cold showers estimated for each family type under uncontrolled and controlled scenarios. As can be seen from Figure 18, the tool cannot further reduce the payback peak detected at 14:30 as the morning control period has reached the maximum limit of 7.5 hours.

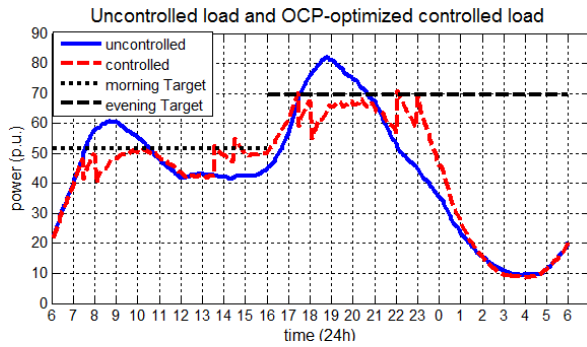


Figure 18. The OCP optimization of a hot water load profile with the dominant evening peak.

Table 6: Probabilities of cold showers for case study 3

	Uncontrolled	Controlled
Family type 1	0.03%	0.05%
Family type 2	4.11%	4.48%
Family type 3	7.50%	8.31%
Family type 4	14.32%	15.81%
Overall	4.82%	5.30%

Comparison of the results produced by the OCP optimizer in the case studies 2 and 3 (Tables 5 and 6) reveals that customers experience similar comfort under different load profiles.

2.6.4 Case Study 4

In this case study, we use the hot water load profile of case study 2 and compare two different switching programs represented in Table 7. Results produced by the OCP optimizer for case study 3 represent the implementation of the default configuration. Results shown in Figure 19 represent the implementation of the second switching program (configuration 2), and Table 8 shows probabilities of cold showers estimated for each family type. The optimized control period is from 07:30 to 13:30 in the morning and from 17:30 to 00:00 in the evening. Peak reductions for morning and evening control periods are 14.8% and 13.2%, respectively.

Table 7: Switching program configurations in case study 4

	Configuration 1 (default)	Configuration 2
Control groups	6	3
Switching Cycle	30 (min)	30 (min)
Control Step	5 (min)	10 (min)
Turn-off periods	5, 10, 15, 20, 25 (min)	10, 20 (min)

Table 8: Probabilities of cold showers for case study 4

	Uncontrolled	Controlled
Family type 1	0.02%	0.08%
Family type 2	4.37%	4.80%
Family type 3	7.96%	8.67%
Family type 4	13.85%	14.55%
Overall	5.06%	5.51%

The default switching program configuration performs slightly better in peak reduction as it has smaller control steps and higher number of control groups. Switching program configuration 2 degrades the customer comfort level further as hot water systems are switched off for longer periods of time.

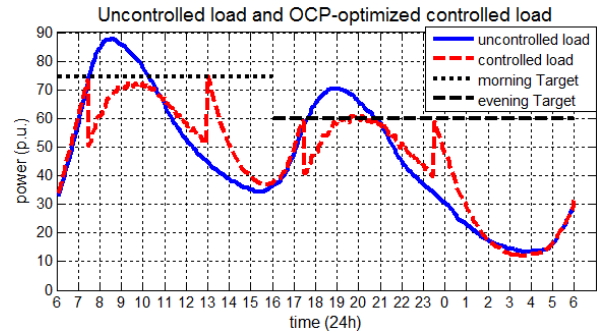


Figure 19. The OCP optimization with the switching program configuration 2.

3 Fast Demand Response for Enabling Higher Penetration of Renewable Energy

Customers living in remote areas often cannot be supplied from conventional interconnected power systems. These customers are usually serviced by a local electricity generation and distribution system with electricity generated using diesel fuel. Due to remoteness and consequent high cost of diesel fuel supply, the cost of electric energy in isolated power systems is high compared to conventional interconnected systems. In some locations, the price exceeds US \$1/kWh, which is an obvious incentive for introducing renewable energy (RE) generation. Unfortunately, RE from the two most abundant energy sources – wind and solar – incurs significant stability and reliability issues due to the intermittency of those sources.

This section presents fast (i.e. sub-second) demand response (DR) as an RE enabling technology in isolated power systems. The advantages of DR are presented, the concept of a fast DR system is discussed, and a case study of the first implementation of the fast DR system, along with some preliminary results, is presented.

3.1 Demand Response in Isolated Power Systems

In general, DR can provide benefits to power systems and their customers by

- Supporting frequency and/or voltage regulation [14], [15];

- Reducing operational costs and emissions by increasing utilization of RE sources [16]. Note that reducing operating costs in turn leads to a greater return on investment which would incentivize expansion of the RE industry;
- Reducing operational costs and emissions caused by traditional generators installed to provide spinning reserve for RE [17];
- Relieving stress from transmission and distribution infrastructure by coordinating loads close to RE sources [17];
- Reducing utility operating costs through advanced metering infrastructure installed to enable DR [18].

Most DR applications focus on large power systems, which have a steady and predictable load profile defined by morning and evening peaks. The time and size of these peak periods can be accurately estimated using historical load data and weather forecasts. In contrast, isolated power systems not only supply less power (MWs, rather than GWs) they are also geographically much smaller. Being smaller in capacity means that demand is less predictable. Being smaller in area means that supply from RE sources is more variable, as a larger percentage of the RE generators are likely to be affected by the same weather events (e.g. a lull in the wind or passing clouds). Due to their reduced demand predictability and increased variability of RE supply, conventional generation scheduling in isolated systems with RE is more challenging. From a generation scheduling perspective - where RE generation is usually treated as a load offset - the daily load curve becomes extremely volatile. An example of an isolated power system (IPS) with RE load curve is given in Figure 20. Notice that it does not even have predetermined daily peaks.

High load variation makes scheduling of diesel generation more difficult and less efficient, as diesel engines will rarely operate at their peak efficiency, and more generator start-ups are required. This is where fast DR can help. It can smooth the variability of required diesel generation by quickly adjusting system load. To be able to do that, fast DR cannot rely on typical load patterns - it must be executed in real-time. If DR is to complement RE in an isolated system, it has to be as fast as the speed at which RE generators change their power output.

3.2 Demand Response as a Virtual Power Plant

The idea of aggregating and controlling small loads to create a large block of variable demand has been discussed in the power engineering literature where it is

often referred to as a ‘virtual power plant’ [19]. Since isolated power systems generally have only one power station, the idea of adding another (virtual) power plant to this system might be a bit misleading. However, isolated systems with RE might have several generating sources (e.g. diesel, wind, solar, etc). Therefore, aggregated DR could be treated as a ‘virtual generator’. Although such a ‘DR Generator’ (DRG) is not generating real power, the power system controller perceives it as one due to the DRG’s ability to decrease the amount of energy needed from other generating sources.

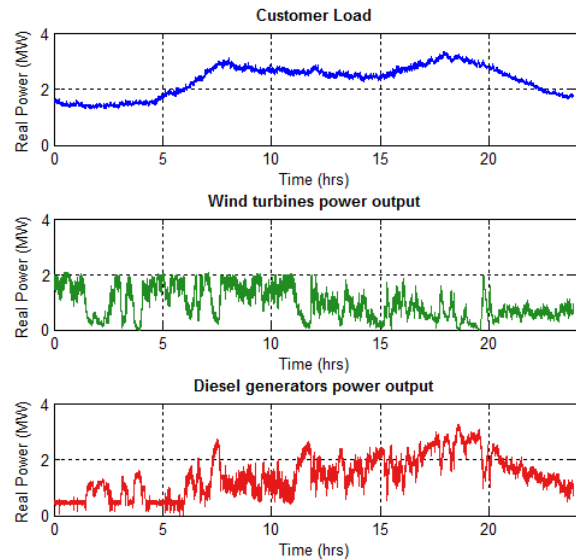


Figure 20. Daily load diagram in an isolated power system.

Isolated systems are usually controlled by a single controller. The controller is typically implemented with a programmable logic controller (PLC). The role of the controller is to schedule available generation in accordance with the current power system constraints, and to maintain system stability. In addition, the controller can be programmed to maximize the amount of RE generation and, consequently, minimize running costs. The controller effectively controls the entire system by collecting data on the current system status and by issuing commands to various generation sources, as shown in Figure 21.

When the controller has a goal to maximize the use of RE, it will dispatch as much renewable generation as the power system can handle while simultaneously maintaining an appropriate level of spinning reserve to ensure system stability. If the amount of RE drops and the system suddenly does not have enough spinning reserve, the controller starts a diesel generator. The role of the DRG is to support higher RE penetration by providing additional spinning reserve. If sufficient

spinning reserve is provided by the DRG, diesel generator start-up is prevented.

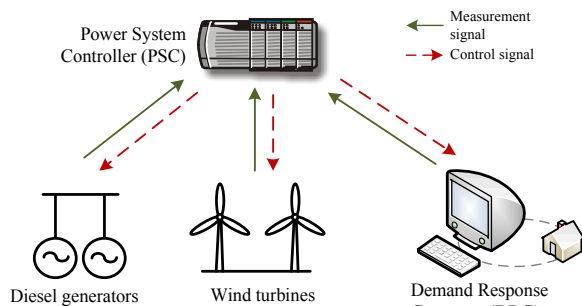


Figure 21. Smart Grid generator in IPS control system.

A DRG consists of three main components, as shown in Figure 22:

- DRG Master controller,
- communications network, and
- slave controllers.

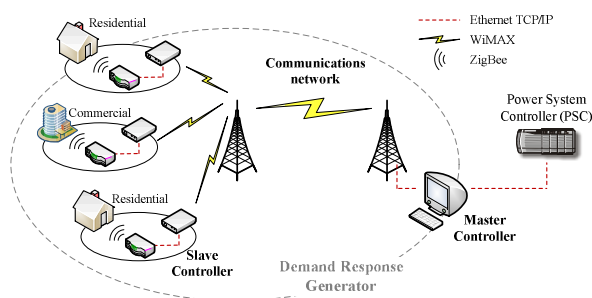


Figure 22. The DRG architecture.

3.2.1 DRG Master Controller

The master controller collects information on available DR and aggregates it into predefined virtual loads (e.g. geographical regions). It constantly communicates available DR capacity to the power system controller (PSC) while checking for DR dispatch requests from the PSC. DR requests identify a target virtual load and the amount of demand to curtail. The master controller selects the individual loads to curtail from the virtual load, and immediately sends a switch-off signal to each.

3.2.2 Communications Network

A multi-protocol bidirectional communications network delivers information between all elements of the DRG. Ethernet is used within the control system. A dedicated WiMAX network provides the backhaul

capability. Within individual customer sites, a WiMAX gateway is connected by Ethernet to a ZigBee gateway for the final link to the load metering and switching devices. This communications configuration is configured to ensure a sub-second round trip for DR requests from the PSC out to the load control devices and back again.

3.2.3 Slave Controllers

Slave controllers are located in each DR capacity providing site. They consist of a pair of gateways to provide WiMAX-Ethernet-ZigBee signal translation between the backhaul network and the individual load control devices. The load control devices perform both metering and load switching. They provide a range of power metrics and also support set-points.

A DRG providing spinning reserve must be extremely responsive and reliable. The master controller must be able to monitor and dispatch slave controllers at all times. This critical requirement becomes obvious in the two most common scenarios:

- If the PSC requests DR for extended periods of time, some slave controllers may override the dispatch as they exceed their maximum dispatch duration. In this situation the master controller must quickly identify and dispatch another device (or devices) with an equivalent load.
- If a slave controller or communication link is unreliable, the DRG may be forced to always dispatch more DR than requested to ensure a suitable margin of error in either load switching or reporting. This is not an efficient use of capacity and may reduce the overall effectiveness of the DRG.

3.3 Case Study

The fast DR technology discussed above was implemented in an IPS as part of the King Island Renewable Energy Integration Project [20]. King Island lies in the Bass Strait between Tasmania and the Australian mainland. It has a population of approximately 2000 people, and an economy based on agriculture and food processing.

3.3.1 The King Island Power System

Customer load on King Island ranges between 1 MW and 3 MW, with an average of around 1.5 MW. The King Island power system is shown in Figure 23. There is one power station on the island with four distribution feeders delivering electricity to customers. The power station houses four diesel generators with a

total generation capacity of 5.8MW. Three fixed speed Nordex N29 (250kW each) wind turbines are installed on a nearby hill, together with two Vestas V52 turbines (850kW each) with doubly fed induction generators. Two 800kW diesel engines with flywheels are also connected to the system. In these generators the flywheels are separated by a clutch from a diesel engine and provide system with additional inertia.

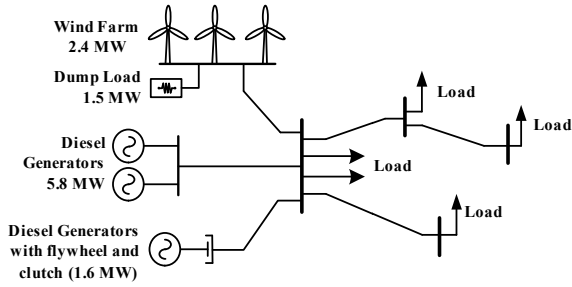


Figure 23. The King Island power system.

3.3.2 The King Island Smart Grid Project

The ongoing King Island Smart Grid project has the goal of supporting higher levels of wind energy integration in the King Island power system by providing:

1. Spinning reserve by implementing the DRG concept, and
2. Fast fine-grained under frequency load shedding (based on the slave controller level).

The master controller constantly monitors the available connected DRG load and passes this information to the PLC-based power system controller. At the same time, the controller monitors the current level of power system spinning reserve. If the spinning reserve falls below a predefined threshold, the controller instructs the DRG to curtail some load and effectively raise the spinning reserve. This function can be observed in Figure 24, where due to a sudden drop in wind generation, the spinning reserve falls. The reduction in spinning reserve causes the power system controller to initiate a request for all available DR, as shown in the lower graph.

The results shown in Figure 24 demonstrate that the implemented DRG was able to respond accurately to given set-points. It also shows that DR capacity can be dispatched reliably in 1 sec.

3.3.3 Preliminary Implementation Results

Currently the King Island DRG has 50 sites under management and has been fully integrated into the power system. When complete, the DRG will be extended to include 150 households and several

commercial loads. Prior to roll-out on King Island, the DRG was tested with 10,000 simulated customer loads with minimal performance degradation [21]. This implies that the full DRG will supply more than 100 kW of sub-second DR capacity.

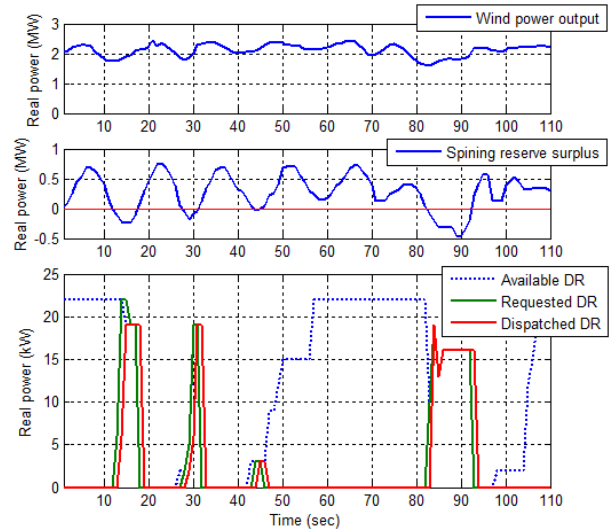


Figure 24. Results of the King Island DRG operation.

The effectiveness of the King Island DRG depends largely on its integration with the power system controller. Figure 25 demonstrate how the controller requests for the DRG and uses it as a tool for regulating demand accurately. During the period of over 2 hours, the King Island power system was running in zero-diesel operation and the DRG was used under small and short dips in wind power generation. In this mode of operation, the power system controller prioritizes DRG dispatch, and thus postpones unnecessary start-ups of a diesel generator.

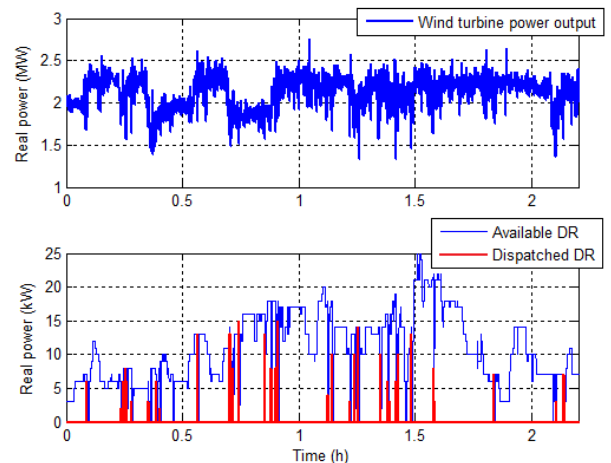


Figure 25. Operation of the King Island DRG.

4 Conclusions

With a strong drive for energy conservation, demand-side management and demand response are becoming vital for the implementation of the smart grid concept. This paper outlines some experience obtained at the University of Tasmania, Australia in developing DSM and DR systems.

The evaluation tool to recommend optimum DSM switching programs for domestic hot water systems has been developed. The tool assesses the performance of a DSM switching program by estimating potential peak load reductions and customer comfort characterized by the probability of cold showers. The starting time and the length of control periods are crucial in peak reduction. However, the length of control periods must be limited to minimize negative impact on customer comfort. The developed tool aims to assist distribution system operators in designing their DSM programs. An operator uses this tool to determine the available domestic water heating load in a controlled area, and predict the potential reduction in peak load. The tool described in this paper has been implemented in the Tasmanian power system since June 2013.

The paper also presented DR as an enabling technology for higher penetration of renewable energy in isolated power systems. These systems are often based on diesel generators. However, due to high costs of diesel fuel supply, the cost of electricity in isolated power systems is much high compared to conventional interconnected systems. This presents an incentive for introducing renewable energy generation in isolated power systems. Unfortunately, the integration of renewable generation presents significant stability and reliability challenges due to their intermittency. The solution proposed in this paper is based on centralized two-way communication and control of residential and commercial loads. DR can be dispatched and confirmed within 1 second. The technology has been installed and successfully tested in an isolated power system on King Island in Australia.

References

- [1] G. Strbac, "Demand side management: Benefits and challenges," *Energy Policy*, vol. 36, pp. 4419–4426, 2008.
- [2] D. T. Nguyen, M. Negnevitsky, and M. de Groot, "Pool-based demand response exchange—concept and modeling," *IEEE Trans. Power Systems*, vol. 26, pp. 1677–1685, 2011.
- [3] K. Heussen, S. You, B. Biegel, L. Hansen, and K. Andersen, "Indirect control for demand side management-A conceptual introduction," in *3rd IEEE PES ISGT Europe*, pp. 1–8, 2012.
- [4] J. Kondoh, "Direct load control for wind power integration," in *IEEE PES General Meeting*, 2011, pp. 1–8.
- [5] S. Elphick, P. Ciufu, and S. Perera, "Supply current characteristics of modern domestic loads," in *Power Engineering Conference, 2009. AUPEC 2009*, pp. 1–6.
- [6] D.I.E.R. of Tasmania. (24 Sep 2013). *Energy in Tasmania*. Available: http://www.dier.tas.gov.au/energy/energy_in_tasmania
- [7] Australian Bureau of Statistics, (01 Nov 2012). Available: www.ausstats.abs.gov.au.
- [8] T. Ohnaka, Y. Tochihara, and Y. Watanabe, "The effects of variation in body temperature on the preferred water temperature and flow rate during showering," *Ergonomics*, vol. 37, pp. 541–546, 1994.
- [9] K. Wong and M. Negnevitsky, "Development of an evaluation tool for demand side management of domestic hot water load," *Proc. IEEE PES GM, Vancouver, Canada*, 21–25 July, 2013.
- [10] Bureau of Meteorology, Australia, (02 Oct 2012). Available: www.bom.gov.au.
- [11] G. van Harmelen, G.J. Delpert, "Multi-Level Expert-Modelling for the Evaluation of Hot Water Load Management opportunities in South Africa", *IEEE Trans Power Systems*, vol. 14, no. 4, pp. 1306–1311, 1999.
- [12] J. Kondoh, N. Lu, and D. J. Hammerstrom, "An evaluation of the water heater load potential for providing regulation service," in *IEEE PES General Meeting*, 2011, pp. 1–8.
- [13] S. Lee and C. Wilkins, "A practical approach to appliance load control analysis: a water heater case study," *IEEE trans. power apparatus and systems*, pp. 1007–1013, 1983.
- [14] J. A. Short, D. G. Infield, and L. L. Freris, "Stabilization of Grid Frequency Through Dynamic Demand Control," *Power Systems, IEEE Transactions on*, vol. 22, pp. 1284–1293, 2007.
- [15] T. L. Vandoorn, B. Renders, L. Degroote, B. Meersman, and L. Vandeveld, "Active Load Control in Islanded Microgrids Based on the Grid Voltage," *Smart Grid, IEEE Transactions on*, vol. 2, pp. 139–151, 2011.
- [16] D. Nikolic, M. Negnevitsky, M. de Groot, et al, "Fast Demand Response as an Enabling Technology for High Renewable Energy Penetration in Isolated Power Systems", *Proc.*

- IEEE/PES General Meeting*, Washington, DC, , 27–31 July, 2014.
- [17] D. Westermann and A. John, “Demand Matching Wind Power Generation With Wide-Area Measurement and Demand-Side Management,” *Energy Conversion, IEEE Transactions on*, vol. 22, pp. 145-149, 2007.
- [18] N. Rajakovic, D. Nikolic, and J. Vujasinovic, “Cost benefit analysis for implementation of a system for remote control and automatic meter reading,” *Proc. PowerTech, 2009 IEEE Bucharest*, 2009, pp. 1-6.
- [19] J. Kumagai, “Virtual power plants, real power,” *Spectrum, IEEE*, vol. 49, pp. 13-14, 2012.
- [20] Hydro Tasmania. (2013). *King Island Renewable Energy Integration Project (KIREIP)*. Available: www.kireip.com.au
- [21] M. de Groot, D. Nikolic and J. Forbes, “Demand Response in Isolated Power Systems,” *Proc. Australasian Universities Power Engineering Conference (AUPEC 2013)*, Hobart, Australia, 2013.